DOI: 10.32615/ps.2020.006 PHOTOSYNTHETICA 58 (SI): 573-584, 2020

Special issue in honour of Prof. Reto J. Strasser

Monitoring seasonal damage of photosynthetic apparatus in mature street trees exposed to road-side salinity caused by heavy traffic

T. SWOCZYNA+ and P. LATOCHA

Department of Environmental Protection and Dendrology, Institute of Horticultural Sciences, Warsaw University of Life Sciences – SGGW, 02-776 Warsaw, Poland

Abstract

De-icing salts are harmful for road-side greenery. The aim of our study was to examine photosystem II performance in mature trees growing along a road of heavy traffic in relation to shoot and soil salinity caused by de-icing salts. Leaves from each three specimens of *Aesculus hippocastanum*, *Tilia cordata*, and *Betula pendula* growing along the same road, nine leaves from a road-side part (RS) and nine from an opposite part (OS) of each tree crown, were sampled in June, July, and September, 2017 and 2018. The PSII performance in RS and OS leaves was compared using chlorophyll *a* fluorescence (ChF) technique. Since the beginning of the both growing seasons, several parameters of ChF were different in OS and RS leaves, especially maximum quantum yield of primary photochemistry and efficiency of electron movement beyond plastoquinone Q_A^- markedly decreased in RS leaves. However, PSII performance was not directly bound to shoot/soil salinity.

Additional key words: JIP-test; performance index; salt stress; traffic pollution.

Introduction

Urban trees play an essential role in mitigating urban air pollution and improving microclimate, therefore they are often called 'amenity trees'. Thanks to their size, they have a great potential of reducing summer temperature due to both direct shading and transpirational cooling (Shashua-Bar and Hoffman 2000, Gillner *et al*. 2015). Their role in urban environment encompasses also carbon dioxide assimilation and sequestration (Nowak and Crane 2002, Yunusa and Linatoc 2018). Trees can also absorb some kinds of air contamination, *e.g.*, sulfur dioxide and nitrogen oxides (Tyrväinen *et al*. 2005). We expect trees will protect us from harsh urban conditions and, on the other hand, they will withstand the conditions they are set by us, humans. The structure of city arrangement and environmental conditions (soil quality, water availability, *etc*.) are often different from natural habitats. Additionally, urban soils and water are often contaminated (Sieghardt *et al*. 2005). Therefore, urban trees often suffer from unfavourable conditions and do not provide expected benefits (Celestian and Martin 2005, Bühler *et al*. 2006).

Although in most of the urban environments the increased air pollution and soil contamination is found (Rogula-Kozłowska *et al*. 2019), trees growing in streets are in particular exposed to contamination coming from vehicle traffic (Dzierżanowski *et al.* 2011). The contamination encompasses heavy metals, volatile organic compounds (VOCs), sulfur dioxide, nitrogen oxides, and others (Majewski and Rogula-Kozłowska 2016). In Central Europe, one of the most detrimental factors affecting urban trees planted along roads are de-icing salts, mostly NaCl, which accumulate in roadside soils (Cekstere *et al*. 2008, Marosz 2011, Swoczyna and Latocha 2016) and on tree shoots during the winter (Borowski *et al.* 2014). Soil salinity affects water uptake due to osmotic constraints and triggers Na^+ and Cl^- uptake by roots (Kalaji and Pietkiewicz 1993). Increased accumulation of Na^+ and Cl^- leads to ion imbalance: ion competition diminishes the uptake, transport, and internal distribution of nutritional elements such as K, Mg, Ca, P, and N (Hu and Schmidhalter 2005). In woody plants, salt ions absorbed by the roots from soil-applied NaCl tend to accumulate in the shoots (Headley and Bassuk 1991, Paludan-Müller *et al.* 2002).

Received 2 September 2019, *accepted* 16 January 2020.
+Corresponding author; e-mail: tatiana_swoczyna@sggw.pl
Abbreviations: ABS – average photon absorption; ChF – chlorophyll *a* fluorescence; DI – energy dissipation; EC – electric conductivity; ET – electron transport; ETC – electron transport chain; F_0 – minimum fluorescence value in a dark-adapted sample; F_m – maximum fluorescence value in a dark-adapted sample; F_v/F_m – maximal quantum yield of PSII photochemistry in a dark-adapted sample; PI – performance index; RC – reaction centre; RE – reduction of end electron acceptors at the PSI acceptor side; TR – excitation trapping.
Acknowledgements: The authors want to thank the Department of Meteorology and Climatology, Warsaw University of Life Sciences – SGGW for climatic data used in this manuscript.

In deciduous trees, salt uptake during dormancy season (winter) is restricted but it rapidly increases with the spring development (Headley and Bassuk 1991). After bud break, Na^+ and Cl^- content increases in leaves, stems, and roots (Paludan-Müller *et al.* 2002), which may be attributed to enhanced water flux through vascular system. It was found that Na^+ concentration in leaves was proportional to salt concentration in the soil (Equiza *et al*. 2017). Salt deposition on shoots was also found to be harmful. Paludan-Müller *et al.* (2002) showed that salt application to bark caused more delayed timing of bud breaking than that applied to buds or bud scales. Nevertheless, buds inside are also affected by salt ion distribution. Jonsson (2006) found a wide range of Cl^- contents in leaf primordia in coastal populations of *Populus trichocarpa* Torr. & Gray despite its buds were covered by 6–7 scales. In his research, terminal bud failure was bound to Cl^- content in leaf primordia and leaf development was adversely related to Cl^- content. Shoot salinity may lead to die-back of terminal shoots when Na^+ and Cl^- content in twigs exceeds particular threshold values (Hofstra and Lumis 1975). In urban environment, salt from shoots is washed down by spring rainfalls, soil salt penetrates down through soil profile, and during the growing season salt concentration in soil is more or less reduced due to precipitation, but simultaneously salt is accumulated in tree tissues through water and ion uptake by roots (Cekstere *et al*. 2008, Hanslin 2011) and it may be stored in trunks and branches for a long time.

Excessive uptake of Na^+ and Cl^- affects cell membrane functioning and cell metabolism by reducing enzyme activities (Kalaji and Pietkiewicz 1993, Gupta and Haung 2014). In response to salt stress, numerous tolerance processes are activated including osmoregulation and ionic stress tolerance, reactive oxygen scavenging, as well as changes in metabolic pathways (Wang *et al.* 2007, Munns and Tester 2008). However, excessive Na^+ and Cl^- contents in cells and tissues lead to disturbances in physiological processes and growth inhibition (Fung *et al.* 1998, Wang *et al.* 2007, Negrão *et al.* 2017). Numerous works showed a decrease of CO_2-fixation rates with increasing concentrations of chloride in leaves of woody species (Downton 1977, Tabatabaei 2006, Wang *et al.* 2007, Sung *et al*. 2010). The effect of salt accumulation in tree tissues causes gradual leaf damage, *i.e.*, marginal chlorosis and necrosis on mature leaves (Cekstere *et al*. 2008). Visible damage in road-side tree leaves was previously described and increased Na^+ and Cl^- contents in leaf tissues were detected (Dmuchowski and Badurek 2004, Cekstere *et al*. 2008). However, the information about the effect of salinity pressure on a photosynthetic apparatus and particularly, PSII performance in leaves of road-side trees is lacking.

Chlorophyll *a* fluorescence (ChF) analysis is a widely used method to analyse the efficiency of PSII and the way to detect the effect of environmental stress in plants. As it is based on optical signals from photosynthetic samples, it is noninvasive and nondestructive to plant tissues. It can inform about plant reactions to different kinds of stress: drought (Fini *et al*. 2009, Wang *et al*. 2012, Guo *et al*. 2016, Kalaji *et al*. 2018a), high temperatures (Srivastava and Strasser 1996, Brestič *et al.* 2012), chilling (Strauss *et al*. 2006), high light (Živčák *et al.* 2015b), salinity (Misra *et al*. 2001, Mehta *et al.* 2010), and N deficiency (Kalaji *et al*. 2014a, Živčák *et al*. 2014, Swoczyna *et al.* 2019). There are two main techniques used. The first one is based on pulse amplitude-modulated (PAM) technique. PAM fluorimeters use both the actinic light, that drives photosynthesis, and the low-intensity measuring light, in order to probe the state of the photosynthetic apparatus (Strasser *et al.* 2000, Kalaji *et al*. 2014b). The second technique is based on application of actinic light also as a measuring light, and is performed using fluorimeters of high-time resolution measurements (with intervals of 10 μs) which enable analysis of an initial rise of ChF after dark adaptation of examined samples (Strasser *et al.* 2000, Kalaji *et al*. 2014b). In this technique, the initial rise of ChF obtained in less than 1 s provides a set of numerous data characterising the state of PSII. Therefore, the latter technique facilitates less time-consuming measurements which are necessary to obtain a large number of samples in a relatively short time (at the same light/temperature conditions). Such an advantage is very useful for field experiments (Fini *et al*. 2009, Johnstone *et al.* 2014, Pollastrini *et al*. 2014, Swoczyna *et al*. 2015, 2019).

The initial rise of ChF after dark adaptation, when shown on a logarithmic time scale, is called a fast (or prompt) fluorescence curve (or transient). This curve with visible points marked as O, J, I, P, according to Strasser and Govindjee (1992), enables to track particular phenomena concerning light absorption and its conversion to biochemical energy. Since Reto J. Strasser and his co-workers developed so called 'JIP-test' (Strasser *et al*. 2000, 2004, 2010), numerous JIP-test parameters were used to describe leaf ontogeny (Jiang *et al*. 2006), to compare examined species varieties, and provenances (Percival *et al*. 2006, Bussotti *et al*. 2010, Swoczyna *et al*. 2015, Kalaji *et al*. 2018b), to assess plant responses to stress (Goltsev *et al*. 2012, Živčák *et al*. 2014, Lin and Jin 2018), to evaluate a role of structural and ecological factors in plant functioning (Johnstone *et al.* 2014, Pollastrini *et al*. 2016), and in other research. The most popular parameters are quantum yields and efficiencies (or probabilities) because of their universal meaning, first of all maximum quantum yield of primary photochemistry (at t_0), φ_{P0}, denoted also as TR_0/ABS or simply as F_v/F_m, followed by efficiency of electron movement into the ETC beyond Q_A^-, ψ_{Eo}, (or ET_0/TR_0), and the efficiency of electron transport until PSI acceptors, δ_{Ro} (or RE_0/ET_0) (Strasser *et al*. 2004, 2010). In some papers, another parameter describing total efficiency of electron transport from PSII to PSI, denoted as ΔV_{IP}, is used (Pollastrini *et al*. 2014, Živčák *et al*. 2015a). It combines efficiency of electron transport up to end electron acceptors of PSI, δ_{R0}, and the efficiency of movement of electron into the electron transport chain beyond Q_A^-, ψ_{E0}, thus is also marked as ψ_{RE0} or RE_0/TR_0.

The overall performance in trees and plants was previously examined using two integrative parameters, so-called performance indices, PI_{ABS} and PI_{total} (Hermans *et al*. 2003, Živčák *et al*. 2014). Some other JIP-test parameters allow assessing any constraints inside or around

PSII. Increased energy dissipation rate per active RC, DI_0/RC, and energy dissipation rate per a given cross section, DI_0/CS_0, may indicate some disturbances in light energy consuming by PSII (Strasser *et al*. 2004). V_K/V_J, reflecting efficiency of electron flow from OEC to PSII RCs (Brestič and Živčák 2013), helps detect drought or thermal stress. Diminished number of active RCs per a given cross section, RC/CS_0, may indicate a photoinhibition effect (Mathur and Jajoo 2014, Živčák *et al*. 2014) or structural disturbances, for example in case of nitrogen deficiency (Swoczyna *et al*. 2019).

The aim of our examination was the evaluation of PSII functioning based on chlorophyll *a* fluorescence technique in road-side tree leaves exposed to higher and lower road contamination pressure dependent on leaf position in a tree crown and an attempt to bound the possible disturbances in PSII performance with salinity pressure affecting road-side trees.

Materials and methods

Plant material: The examination was conducted in Warsaw (52°10'N, 21°02'E) along Dolina Służewiecka, an arterial road of heavy traffic. During the winter, de-icing actions are performed there in case of snowing as in most other streets in Warsaw using the NaCl water solution. The salt solution is sprayed only on the road surface excluding roadside lawn strips, however, heavy car traffic causes dispersal of salt aerosol to neighbouring surfaces. Mature trees of three species, *Aesculus hippocastanum* L., *Tilia cordata* Mill., and *Betula pendula* Roth., were examined. We took advantage of the fact that trees of three different species grow along the same road and we assumed the trees are influenced by the same microclimatic and soil conditions. Three specimens of each species without any symptoms of damage caused by pests or pathogens were chosen for the analysis. *Tilia* and *Aesculus* trees grew in one row along the road, in a distance of 2.60 and 4 m, respectively. *Betula* trees grew in two rows with a space of 3 m from the road and 4 m between them, having tree crowns overlapping. Examined *Tilia* trees were 8–10 m high and 7–9 m of crown width, with a girth in the range of 62–94 cm. *Aesculus* trees were 7.5–8 m high, with a width of 7–8 m and a girth of 91–97 cm. *Betula* trees in the first road-side row were 10–12 m high, with a width of 7–7.5 m and a girth of 62–94 cm, trees in the second row were 12–13 m high, with a width of 8–11 m and a girth of 94–116 cm. *Tilia* and *Aesculus* crown edges reached the road area, in *Betula*, bottom crown edges were *ca*. 40–50 cm apart the road edge. In all the examined trees die-back symptoms of road-side twigs were visible at the road-side part of tree crowns and each year new shoots were developed there (photographs not available).

Shoot and soil salinity: On 14 March 2017, *i.e*., before bud swelling, alive shoots from a road-side part of tree crowns (RS) and shoots from an opposite side of the crowns (OS) were collected (cut off) from each tree (two samples, RS and OS, from each tree) from the height of 1.5–2.5 m above the ground. Due to great differences in shoot diameter in examined species, each sample consisted of 5, 10, and up to 30 shoots from *Aesculus*, *Tilia*, and *Betula*, respectively. In *Betula*, RS samples were taken from road-side trees and OS samples were obtained from the parallel trees from the second row. In order to assess magnitude of shoot and soil salinity in examined trees, additional specimens of *Betula pendula*, *Tilia cordata*, and *Aesculus hippocastanum* growing in the neighbourhood but in the greater distance from the road (12–40 m apart from any road edge) were chosen. The reference trees (Ref trees) were 8–10 m high, with a width of 6–8 m and a girth of 39–85 cm. *Aesculus* and *Betula* reference trees from the neighbourhood grow in different site conditions, both soil and microclimatic, not in rows in an open space but in groups, so their ChF results could be influenced by numerous undefined factors. We used the Ref trees only to evaluate the level of soil and shoot salinity affecting examined trees and we did not measure ChF on their leaves.

The diameter of each shoot was measured *ca*. 4 cm below the apical bud. Shoots with wounds were absolutely excluded in order to avoid sap leakage. Shoot diameters were within the range of 0.47–1.06, 0.16–0.36, and 0.08–0.33 cm in *Aesculus*, *Tilia*, and *Betula*, respectively. Approximated surface of every shoot was calculated as a right circular cylinder surface by multiplication of circumference of a shoot (calculated from a measured shoot diameter) by length of 6.5 cm (as the cylinder height).

Apical parts of every shoot sample were immersed in 120 cm^3 distilled water at 20°C for the depth of 6.5 cm in separate beakers and moved three times to provide better salt washing out. After 1 h shoots were removed and the electric conductivity of the solutions was measured using a *CX-551* multifunction meter (*ELMETRON Sp.j*., Zabrze, Poland). Salinity of the solutions depended not only on a real salt deposition on the shoots but also on the total shoot area in the samples. Therefore, shoot salinity was calculated as a standardised salinity coefficient Z: $Z = EC/Area$, where EC [$mS\ cm^{-1}$] is electrical conductivity of a solution obtained from each sample, Area [cm^2] is the sum of approximated surfaces of shoots being the single sample. For better visualisation in a statistical graph the coefficient Z was multiplied by 1,000.

Additionally, soil EC was measured at both sides of the tree trunks (in case of *Betula*, road-adjacent tree trunks). Soil samples were taken at 0–20 cm depth approximately 1 m apart from a tree trunk from the road-adjacent side (RS) and the opposite side (OS) of each tree trunk or around the tree trunk in Ref trees. Samples were collected on 23 May, 28 June, and 29 August 2017 and taken to the laboratory. Soil samples were air-dried, then diluted in distilled water (1:2, soil:water volumetric ratio), left for 18 h and their electrical conductivity was measured using a *CX-551* multifunction meter (*ELMETRON Sp.j.*, Zabrze, Poland). The results were multiplied by three in order to obtain the accurate soil EC.

Chlorophyll *a* fluorescence measurements were performed on leaves collected between 9:00 and 10:00 h on 16 June, 31 July, 13 September 2017; and 5 June, 31 July, 4 September 2018. Nine shaded leaves were picked up

from the road-side part of a tree crown (RS) and nine shaded leaves from the opposite side of a tree crown (OS) from the height of 1.50–2.50 m from three trees of each species (27 leaves per treatment in each species). Leaves were collected from the height of 1.5–2.5 m above the ground, put into paper bags and to an additional textile bag, and immediately (within 30 min) transported to the laboratory for the measurements.

Fast kinetics of ChF was measured using a *HandyPEA* fluorimeter (*Hansatech Instruments Ltd*., King's Lynn, Norfolk, Great Britain). Leaves were dark-adapted using light-excluding clips for 25 min. The dark-adapted leaf samples of 4-mm diameter within each clip were illuminated with 660-nm light of 3,444 μmol(photon) m^{-2} s^{-1}.

Based on ChF measurements, the following parameters of the JIP-test were calculated: density of active RCs (Q_A reducing RCs) per cross section at point 0, RC/CS_0, energy dissipation rate per cross section of the sample at point 0, DI_0/CS_0, energy dissipation rate per active reaction centre of PSII, DI_0/RC, quantum yields and efficiencies, φ_{P0} ($= F_v/F_m$), ψ_{E0}, δ_{Ro}, total efficiency of electron transport from PSII to PSI, ΔV_{IP}, the ratio of variable fluorescence at 300 μs and variable fluorescence at 2 ms, V_K/V_J, and performance indices, PI_{ABS} and PI_{total}. All the examined parameters are explained in the Appendix.

Statistical analysis: *Student*'s test *t* was performed on data from each species and date in order to compare the PSII performance in RS and OS leaves on each measurement date. A principal component analysis (PCA) was performed on a correlation matrix of the means from RS and OS leaves and of three species. ChF parameters from each date were analysed separately. In PCA of both June and September 2017 results, the average annual value of soil EC for each sampled site (OS or RS) was used. The PCA graphs were plotted automatically by a software. Correlation analysis was performed for the results from June and September 2017. For the correlation analysis of the measurements taken in June, we used average values of ChF parameters from nine records on each tree and each side of the crown (six values per species, 18 values in total), the calculated coefficient Z from each tree multiplied by 1,000 (six values per species, 18 values in total), and average values of soil EC from three sampling dates for each species (two values per species, six values in total). All calculations and PCA graphs were made using *STATISTICA ver. 13.3* software (*TIBCO Software Inc. (2017)*, http://statistica.io., USA).

Results

Shoots collected from the road-side part of tree crowns showed the highest surface salinity (Fig. 1*A*). However, shoots from the opposite part of tree crowns were also covered with salt to a greater extent than that in the reference trees growing apart from the road.

In general, soil salinity measured as EC was higher in the close proximity to the road than that in a distance of 3.6–5 m (Table 1). In May and August, EC was markedly higher in soils around *Aesculus* reference trees situated in a great distance from the road. There were some cases when soil EC in August was higher than that in July and this might be explained by precipitation deficiency in August (68.5 mm compared to 106.2 mm and 111 mm in June and July, respectively; Fig. 1*B*) leading to higher ion concentrations in the soils.

The ChF transient in June 2017 showed only minor differences between OS and RS leaves (Fig. 2*A*). In September, maximal fluorescence in RS leaves was visibly lower (Fig. 2*B*). As shown in the Fig. 2*C*, fast fluorescence transient in RS leaves revealed a marked shift in comparison to the transient in OS leaves normalised to 0. (Additional ChF transients are shown in Fig. 1S, *supplement*.) Since the beginning of the growing season several parameters of JIP-test were different in OS and RS leaves both in 2017 and 2018. In particular, φ_{P0} and ψ_{E0} markedly decreased in RS leaves (Tables 2, 3). PI_{ABS}, a parameter dependent on φ_{P0} and ψ_{E0}, was also significantly lower in RS leaves in most cases. The highly visible effect of road-side pressure was noted in DI_0/RC, as well. In 2018, the most affected by road-side pressure species was *Aesculus*, particularly in September all ChF parameters were different in this species (Table 3). Some parameters in RS leaves in *Aesculus* were not only significantly lower/higher than in OS leaves, but also reached the lowest (φ_{P0}) or the highest (DI_0/RC) values in all the samples at any date. DI_0/RC and φ_{P0} were also the most often differing parameters in *Tilia* and *Betula*.

In the PCA performed on 2017 results, PC 1 had large associations with ChF parameters, so this component reflected the PSII physiological condition. The PC 2 had large associations with soil and shoot EC, so this component reflected the pressure of road-side contamination. In June, most of ChF parameters were not directly bound to PC 2. However, the slopes of ψ_{E0} and RC/CS_0 suggest some kind of pressure of road-side stress on these parameters,

Table 1. Soil electric conductivity [mS cm^{-1}] in soil samples collected from 1.60–3 m apart from the road (RS), 3.60–5 m apart from the road (OS), and from 12–40 m apart from any road (Ref).

	Aesculus hippocastanum			*Betula pendula*			*Tilia cordata*		
	RS	OS	Ref	RS	OS	Ref	RS	OS	Ref
23 May	1.04	0.63	0.91	1.29	0.60	0.59	1.41	1.20	0.83
28 June	0.72	0.68	0.65	1.06	0.56	0.51	0.73	0.50	0.52
29 August	1.43	0.68	0.85	0.84	0.51	0.64	0.84	0.71	0.77
Average	1.06	0.66	0.80	1.07	0.56	0.58	0.99	0.80	0.70

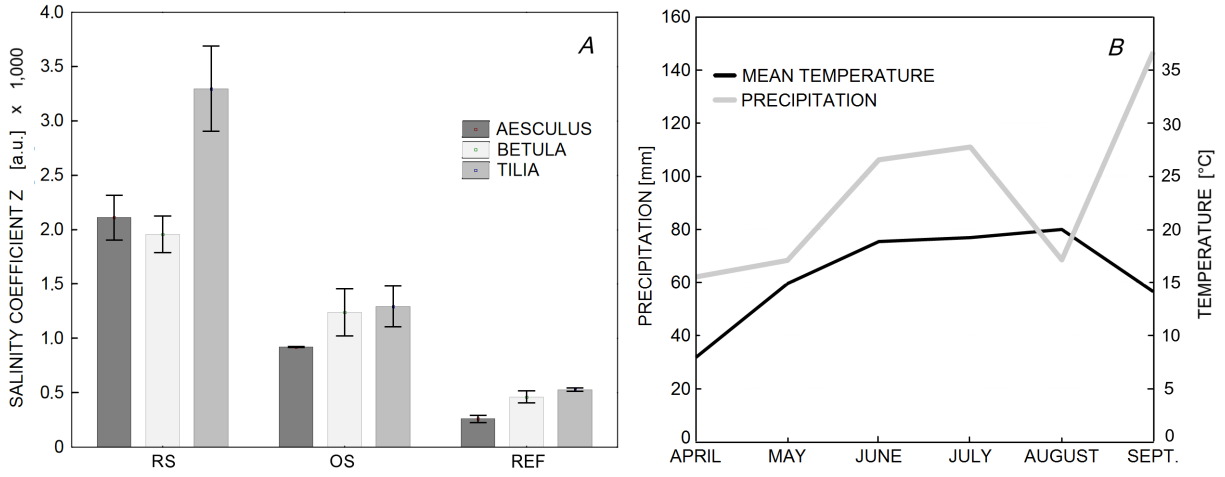

Fig. 1. (*A*) Standardised shoot salinity coefficient Z calculated as a ratio of EC of diluted salt spray from shoots divided by approximated area of shoot surface. For better visualisation in a statistical graph, the coefficient Z was multiplied by 1,000. Means ± SE, n = 3. RS – shoots collected from a road-side part of tree crowns, OS – shoots from an opposite side of the crowns, REF – shoots collected from reference trees growing in a greater distance from a road. (*B*) Mean monthly temperature and precipitation in the growing season 2017.

the higher pressure the lower ψ_{E0} and RC/CS_0 values (Fig. 3*A*). The slopes of the lines connecting RS and OS in *Betula* and *Tilia* suggest that the PC 2 might affect some parameters of PSII performance, namely ψ_{E0}, RC/CS_0, and to some extent PI_{ABS} in young leaves (Fig. 3*B*).

In September, maximum quantum efficiency (φ_{P0}) was adversely bound to the PC 2 to a greater extent. Both DI_0/CS_0 and DI_0/RC lines were closer to soil EC line suggesting the increasing effect of soil salinity on dissipation rate in the end of the growing season (Fig. 3*C*). The slopes of the lines connecting RS and OS in *Betula* and *Aesculus* indicate the relationship between some parameters of ChF, especially φ_{P0}, DI_0/CS_0, and DI_0/RC and the road-side pressure (Fig. 3*D*).

The correlation analysis showed no significant relationships between salinity and ChF parameters (Table 4). Both the *Pearson*'s correlation coefficient and the *p*-value showed very weak connections between PSII condition and soil EC or shoot salinity coefficient Z.

Discussion

Soil salinity in road-side soils is caused by application of de-icing salts in order to facilitate proper conditions for road traffic, thus the highest salt concentration in road-side soils is in the end of winter and afterwards it gradually decreases (Cekstere *et al*. 2008). We have expected that our results from EC measurements in 2017 would confirm the findings of previous works. But in some cases, EC measurements in August showed higher values than that in June. The sparse precipitation in August might be the reason for these results, noted also in reference trees, which were not affected by any salt application. When soil water was lacking, the total concentration of soil ions might have increased giving such unexpected shifted EC values (van der Zee *et al.* 2014). Nevertheless, the soil salinity around examined trees was not the same, the road-side part of root system was evidently exposed to higher salinity. The area on the opposite side of the tree trunks, 3.60–5 m away from a road edge, revealed moderate salinity, reflected by EC not exceeding 0.7 mS cm^{-1}, except *Tilia* trees, where 1.2 mS cm^{-1} was noted in May.

Results of shoot salinity confirmed previous findings indicating higher salt deposition on shoot exposed directly to road traffic (Berkheimer and Hanson 2006, Borowski *et al*. 2014). We found that salt deposition on shoots in road-side parts of tree crowns was twice as high as that at the opposite side. Borowski and Pstrągowska (2010) described harmful effect of salt deposition on shoots on bud breaking, leaf ontogeny, and visible tree conditions. They ascertained high mortality of road-side buds leading to crown deformations. We have assumed that increased salt deposition on shoots and buds just before bud breaking would result in changes in PSII performance of newly developed tissues.

Our two-year examination showed significant changes in PSII performance between leaves collected from road-side parts of tree crowns and from the opposite side. In the first decade of June, leaves of all species reached a maturity stage. ChF transients of both RS and OS leaves obtained on 16 June 2017 did not differ much in shape (Fig. 2*A*). However, some divergences at point K and J are visible when plotting RS results normalised to OS values (Fig. 2*C*). These divergences in *Betula* and *Tilia* prolonged during the growing season (however, not markedly significant in V_K/V_J, 0.064 and 0.059, in *Betula* and *Tilia*, respectively) indicating diminished maximum quantum efficiency of PSII and some disturbances in a water-splitting complex in RS leaves. Moreover, the efficiency of electron movement into the ETC beyond Q_A^-, was also diminished in RS leaves. In the late growing season of 2017, the negative effect of road-side pressure was still visible in *Betula* and *Tilia*, and on that date, the diminished φ_{P0} and ψ_{E0} values were also noted in *Aesculus* (Table 2).

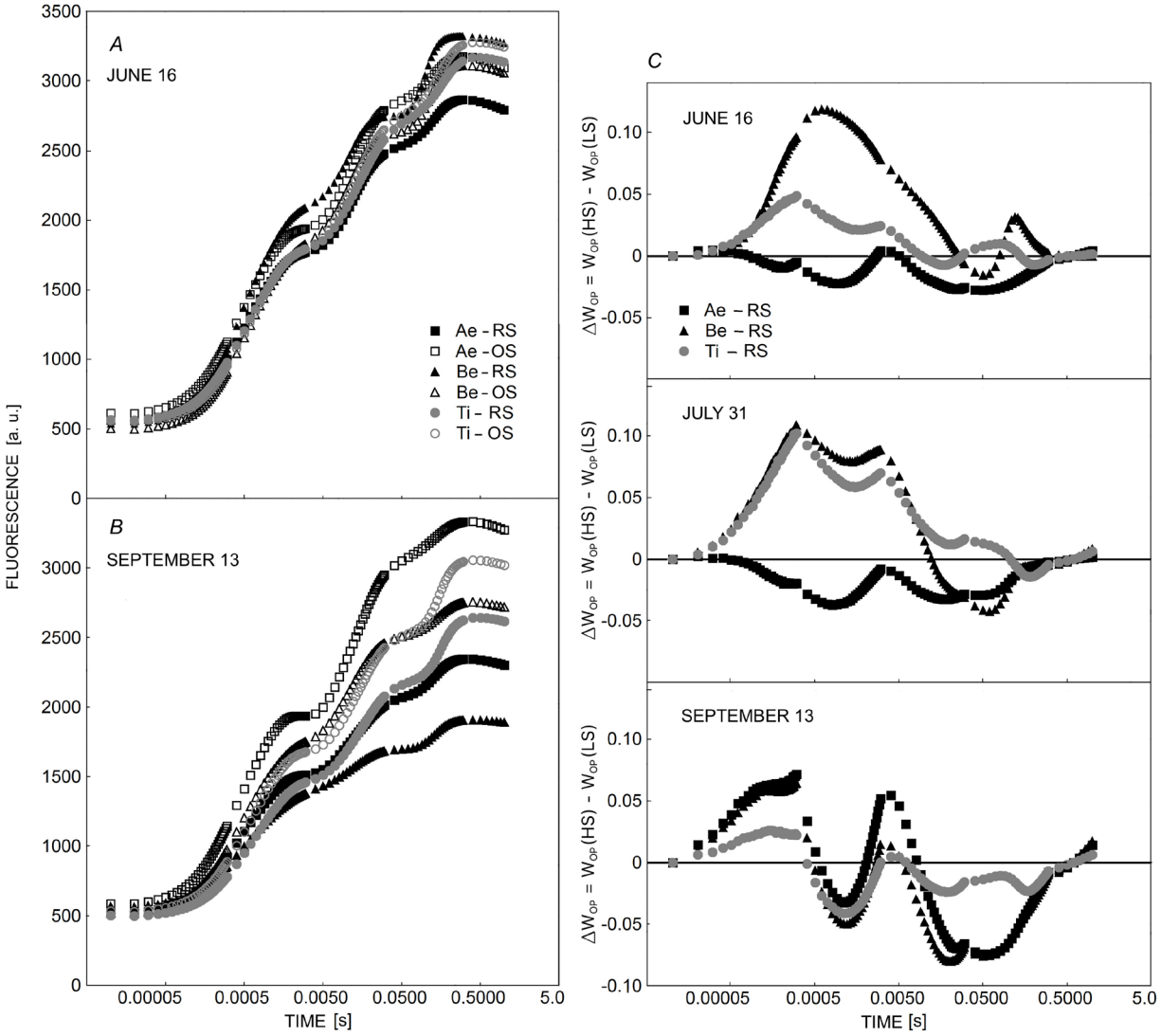

Fig. 2. Fluorescence transient in leaves from a road-side part (RS) and from an opposite part (OS) of tree crowns, 16 June (*A*) and 13 September (*B*), 2017. (*C*) Change in the shape of the chlorophyll *a* fluorescence transient curves normalised between F_0 and F_m expressed as W_{OP} [$W_{OP} = (F_t - F_0)/(F_m - F_0)$], related to corresponding OS of *Aesculus hippocastanum* (Ae), *Betula pendula* (Be), and *Tilia cordata* (Ti) (a horizontal line at 0), 2017.

The similar results were obtained in 2018, however, not identical (Table 3). This indicates that the pressure of road-side conditions affects seriously performance of RCs (Strasser *et al*. 2004, Brestič and Živčák 2013), as well as disturbs redox processes between electron carriers, *i.e*., plastoquinones Q_A^-, and Q_B^- (Strasser *et al*. 2004, Mehta *et al*. 2010).

Another parameter confirming the disturbances in RCs was DI_0/RC. The significantly higher DI_0/RC in most cases indicates the appearance of inactivation of some amount of RCs (Strasser *et al*. 2000). In this case, a smaller pool of active reaction centres acts then as 'a bottle neck' for energy conversion. When the light energy cannot be sufficiently converted to biochemical energy, some part of it is dissipated as heat giving shifted DI_0/RC values. The appearance of the increased dissipation in RS leaves was also confirmed by similar results of DI_0/CS_0 shown in the PCA graph (Fig. 3*A*,*C*). The integrative parameter, PI_{ABS}, also revealed significant differences between OS and RS leaves. As it combines three components, it allows detecting any differences between samples even though other parameters may not be significant individually. Thus it is helpful in detecting the stress occurrence in environmental studies (Hermans *et al*. 2003, Pollastrini *et al*. 2016). In our examination, it was the third sensitive parameter following φ_{P0} and DI_0/RC.

The adverse results were found in δ_{R0}. This parameter revealed higher values in RS leaves always when significantly differed (Tables 2, 3). Such results indicating higher probability of electron flow through end electron acceptors (carriers) at PSI in RS leaves were found in previous works concerning heat stress (Brestič *et al*. 2012, Duan

Table 2. Chlorophyll *a* fluorescence parameters in leaves from a road-side part (RS) and from an opposite part (OS) of tree crowns, 2017. For each parameter *Student*'s test *t* was performed and the *p*-value is shown. V_K/V_J – efficiency of electron flow from OEC to PSII reaction centres, DI_0/RC – energy dissipation rate per active reaction centre of PSII, φ_{P0} – maximum quantum yield of PSII photochemistry, ψ_0 – efficiency (probability) of an electron movement into the electron transport chain beyond Q_A, δ_{R0} – probability that an electron from the intersystem electron carriers is transferred to reduce end electron acceptors at the PSI acceptor side, ΔV_{IP} – total efficiency of electron transport from PSII to PSI, PI_{ABS} – performance index for energy conservation from photons absorbed by PSII to the reduction of intersystem electron acceptors, PI_{total} – performance index for energy conservation from photons absorbed by PSII to the reduction of PSI end electron acceptors, RC/CS_0 – density of active reaction centres per cross section at point 0.

	Aesculus hippocastanum			*Betula pendula*			*Tilia cordata*		
	OS	RS	*p*	OS	RS	*p*	OS	RS	*p*
16 June									
V_K/V_J	0.421	0.399	0.014	0.350	0.387	0.000	0.359	0.375	0.095
DI_0/RC	0.300	0.290	0.258	0.201	0.218	0.000	0.222	0.248	0.008
φ_{P0}	0.824	0.821	0.196	0.853	0.855	0.089	0.844	0.835	0.000
ψ_0	0.484	0.428	0.874	0.517	0.460	0.000	0.557	0.541	0.084
δ_{R0}	0.305	0.342	0.000	0.376	0.445	0.000	0.407	0.412	0.598
ΔV_{IP}	0.148	0.165	0.003	0.194	0.204	0.056	0.226	0.223	0.649
PI_{ABS}	2.656	2.766	0.566	4.580	3.399	0.000	4.882	4.168	0.014
PI_{total}	1.171	1.449	0.016	2.751	2.756	0.976	3.369	2.953	0.077
RC/CS_0	327.7	318.8	0.223	335.2	319.5	0.009	362.1	351.5	0.210
31 July									
V_K/V_J	0.439	0.416	0.063	0.379	0.403	0.064	0.353	0.370	0.059
DI_0/RC	0.302	0.307	0.737	0.217	0.282	0.000	0.212	0.254	0.000
φ_{P0}	0.829	0.820	0.030	0.853	0.828	0.000	0.847	0.829	0.000
ψ_0	0.509	0.519	0.422	0.532	0.463	0.000	0.593	0.549	0.000
δ_{R0}	0.273	0.309	0.004	0.313	0.407	0.000	0.403	0.391	0.264
ΔV_{IP}	0.138	0.160	0.001	0.165	0.187	0.000	0.239	0.216	0.003
PI_{ABS}	3.013	3.167	0.588	4.728	2.849	0.000	5.941	4.190	0.000
PI_{total}	1.128	1.413	0.031	2.099	1.886	0.218	4.032	2.785	0.000
RC/CS_0	298.7	305.6	0.409	297.5	295.1	0.782	358.1	340.8	0.031
16 September									
V_K/V_J	0.440	0.429	0.517	0.410	0.436	0.173	0.345	0.331	0.046
DI_0/RC	0.276	0.367	0.000	0.292	1.979	0.002	0.223	0.244	0.043
φ_{P0}	0.842	0.797	0.000	0.826	0.625	0.000	0.838	0.820	0.000
ψ_0	0.497	0.460	0.009	0.463	0.358	0.000	0.555	0.570	0.154
δ_{R0}	0.278	0.394	0.000	0.283	0.326	0.122	0.442	0.457	0.081
ΔV_{IP}	0.138	0.180	0.000	0.130	0.129	0.947	0.245	0.261	0.058
PI_{ABS}	3.150	2.148	0.000	2.809	1.412	0.000	4.886	4.760	0.737
PI_{total}	0.392	0.666	0.000	0.400	0.531	0.015	3.912	4.080	0.672
RC/CS_0	305.0	271.3	0.002	290.6	239.2	0.020	361.0	350.7	0.162

et al. 2015) and N deficiency (Swoczyna *et al*. 2019). This parameter is included in PI_{total}. Therefore, the values of PI_{total} were mitigated to some extent by δ_{R0} values and the differences between OS and RS leaves were in many cases not significant. Likewise, ΔV_{IP}, as combining contrary results of δ_{R0} and ψ_{E0}, was a weaker indicator of the road-side pressure.

Surprisingly, the correlation analysis as well as the PCA performed on the results from the 2017 growing season did not show strong connections between the most of the ChF parameters and the soil or shoot salinity. In the PCA, numerous ChF parameters located along *x*-axis indicate the overall PSII condition or performance as the PC 1. Parameters concerning dissipation are at the opposite side than φ_{P0}, PI_{ABS}, and PI_{total}, which is quite obvious. Salinity parameters are located along *y*-axis, thus they are markedly bound to the PC 2. However, as it has been shown by correlation analysis, the ChF parameters were not directly dependent on soil salinity nor on shoot salinity. Therefore, the PC 2 should be identified as a complex road-side pressure rather than as the salinity pressure.

The directions of RC/CS_0 and ψ_{E0} lines suggest some adverse relation occurring between these parameters and the road-side pressure (Fig. 3*A*). This suggests that in the early growing season, the road-side pressure might have disturbed performance of electron carriers, plastoquinones

Table 3. Chlorophyll *a* fluorescence parameters in leaves from a road-side part (RS) and from an opposite part (OS) of tree crowns, 2018. For each parameter *Student*'s test *t* was performed and the *p*-value is shown. For parameters explanations, *see* Table 2.

	Aesculus hippocastanum			*Betula pendula*			*Tilia cordata*		
	OS	RS	*p*	OS	RS	*p*	OS	RS	*p*
5 June									
V_K/V_J	0.409	0.414	0.625	0.377	0.382	0.638	0.353	0.386	0.004
DI_0/RC	0.268	0.288	0.023	0.210	0.213	0.789	0.203	0.256	0.001
φ_{P0}	0.836	0.827	0.003	0.857	0.857	0.901	0.853	0.837	0.000
ψ_0	0.547	0.524	0.018	0.540	0.542	0.901	0.609	0.571	0.004
δ_{R0}	0.274	0.274	0.000	0.377	0.369	0.555	0.361	0.349	0.296
ΔV_{IP}	0.150	0.150	0.003	0.204	0.201	0.749	0.220	0.201	0.042
PI_{ABS}	3.880	3.315	0.018	4.948	5.260	0.523	6.669	5.002	0.001
PI_{total}	1.479	1.567	0.440	2.986	3.206	0.521	3.802	2.806	0.003
RC/CS_0	327.2	282.2	0.000	306.4	308.2	0.851	365.0	340.5	0.001
31 July									
V_K/V_J	0.474	0.475	0.961	0.384	0.428	0.000	0.372	0.390	0.060
DI_0/RC	0.294	0.408	0.000	0.218	0.277	0.000	0.236	0.289	0.001
φ_{P0}	0.843	0.800	0.000	0.855	0.838	0.000	0.840	0.820	0.000
ψ_0	0.541	0.496	0.001	0.554	0.491	0.000	0.601	0.565	0.000
δ_{R0}	0.205	0.296	0.000	0.303	0.345	0.002	0.382	0.387	0.673
ΔV_{IP}	0.111	0.144	0.000	0.169	0.169	0.983	0.229	0.218	0.142
PI_{ABS}	3.504	2.381	0.000	5.013	3.265	0.000	5.516	4.017	0.000
PI_{total}	0.920	0.921	0.996	2.229	1.727	0.019	3.391	2.529	0.000
RC/CS_0	273.5	249.9	0.012	285.7	250.3	0.000	328.5	311.8	0.029
4 September									
V_K/V_J	0.400	0.466	0.000	0.317	0.310	0.550	0.295	0.319	0.008
DI_0/RC	0.286	0.717	0.000	0.205	0.230	0.060	0.201	0.253	0.002
φ_{P0}	0.824	0.700	0.000	0.838	0.821	0.000	0.831	0.811	0.001
ψ_0	0.498	0.403	0.000	0.523	0.502	0.159	0.584	0.553	0.008
δ_{R0}	0.211	0.363	0.000	0.301	0.378	0.000	0.395	0.390	0.651
ΔV_{IP}	0.105	0.145	0.000	0.158	0.190	0.001	0.231	0.215	0.046
PI_{ABS}	2.970	1.003	0.000	4.741	4.329	0.432	6.007	4.573	0.001
PI_{total}	0.784	0.516	0.001	2.066	2.707	0.073	3.985	2.946	0.003
RC/CS_0	146.2	103.4	0.000	152.0	149.6	0.643	189.2	168.0	0.000

Q_A^- and Q_B^-, and negatively affected formation or activity of RCs. These findings concern particularly *Betula* and *Tilia* (Fig. 3*B*). In the late growing season 2017, parameters characterising PSII performance were not highly bound to salinity parameters as well (Fig. 3*C*). The slopes of the lines connecting RS and OS in the Fig. 3*D* suggest that in the end of the growing season, the road-side pressure might influence performance of PSII to a greater extent, especially φ_{P0}, particularly in *Aesculus* and *Betula*.

Soil salinity was previously shown as a harmful factor affecting the condition of photosynthetic apparatus (Misra *et al*. 2001, Mehta *et al*. 2010, Kalaji *et al*. 2018a). It was found that Na^+ and Cl^- ions are accumulated in tree tissues, including trunk, branches, and roots, and later distributed to newly emerging organs like shoots, leaves, flowers, *etc*. (Paludan-Müller *et al*. 2002). Despite of spring rainfalls and decreasing soil salinity during the growing season, the Na^+ and Cl^- content in leaves increases (Cekstere *et al*. 2008). As ion accumulation in leaves takes place indirectly *via* other tissues, we can assume that ions are more or less evenly distributed to all directions in a tree crown. Previous papers indicate that salt aerosol covering twigs, shoots, and buds in road-side or growing in coastal sites trees or shrubs (or plants in coastal sites) evokes die-back of those organs (Berkheimer *et al*. 2006, Jonsson 2006). Cl^- ions are present in a salt film covering buds; they can penetrate through bud scales and are deposited in leaf primordia (Jonsson 2006). Afterwards they may be still present in newly developed leaves (Paludan-Müller *et al*. 2002).

Nevertheless, although we observed shoot die-back and leaf chlorosis and necrosis in the road-side parts of tree crowns, we did not ascertained the clear relationship between the decrease of PSII performance and salinity parameters. Here two explanations are possible. (*1*) Even though we collected leaves with chlorosis and/or necrosis,

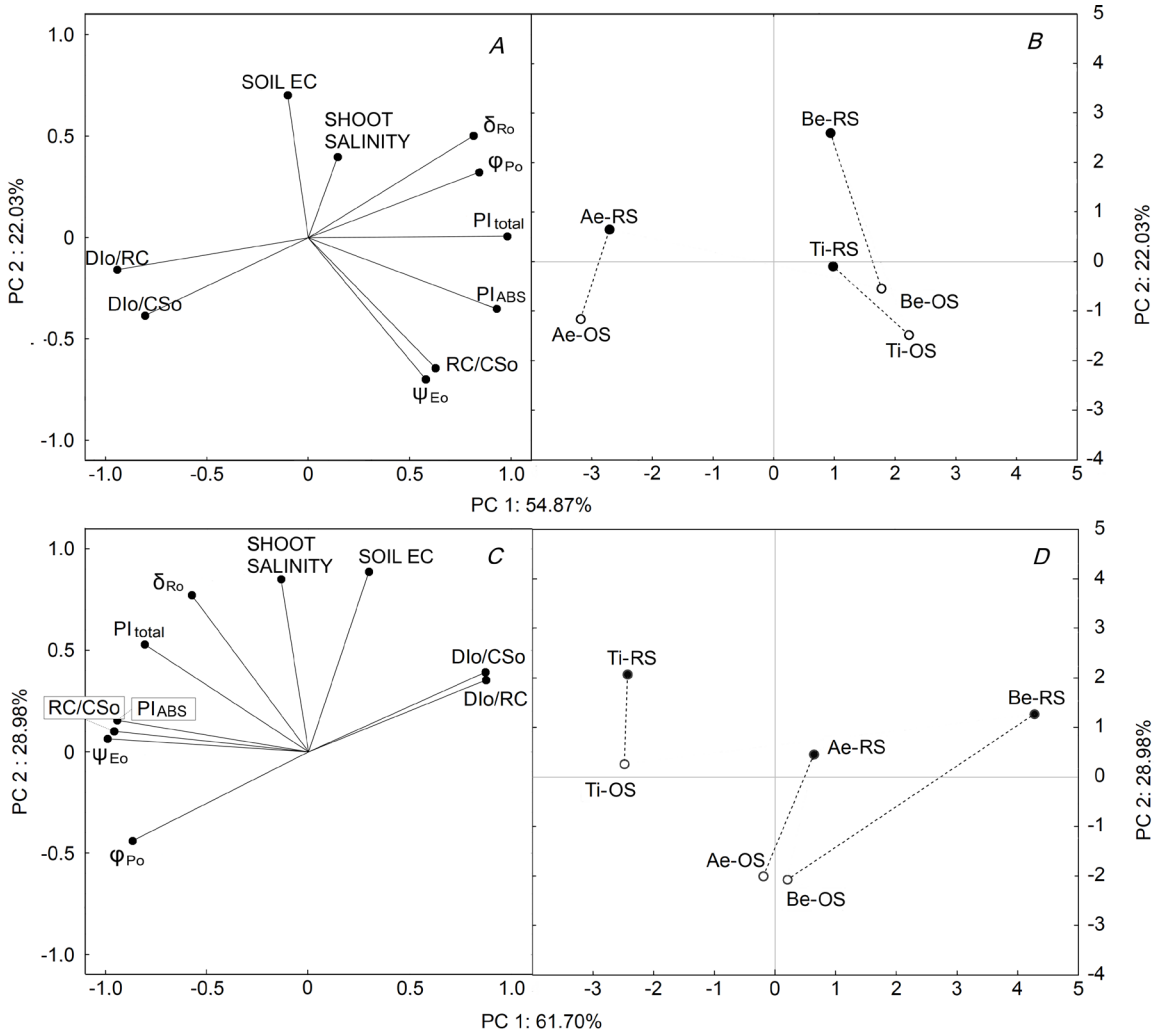

Fig. 3. Principal Component Analysis on ChF and salinity parameters obtained in the early (16 June; *A*,*B*) and late (13 September; *C*,*D*) growing season 2017 in leaves collected from a road-side part (RS) and from an opposite part (OS) of tree crowns. Ae – *Aesculus hippocastanum*, Be – *Betula pendula*, Ti – *Tilia cordata*.

Table 4. *Pearson*'s correlation coefficient *r* and significance level *p* in correlation analysis of ChF parameters, the calculated shoot salinity coefficient Z multiplied by 1,000 and soil EC. For the analysis ChF parameters from nine records on each tree and each side of the crown (six values per species, 18 values in total) taken on the given date, the calculated coefficient Z from each tree multiplied by 1,000 (six values per species, 18 values in total), and average values of soil EC from three sampling dates for each species (two values per species, six values in total) were used. For parameters explanations, *see* Table 2.

	June 2017				September 2017			
	Soil EC		Shoot salinity coefficient Z		Soil EC		Shoot salinity coefficient Z	
	r	*p*	*r*	*p*	*r*	*p*	*r*	*p*
V_K/V_J	0.185	0.462	–0.058	0.819	–0.103	0.685	–0.341	0.166
DI_0/RC	0.159	0.467	–0.011	0.966	0.251	0.316	0.036	0.886
φ_{P0}	–0.138	0.584	–0.045	0.861	–0.326	0.186	–0.081	0.748
ψ_0	–0.247	0.323	0.046	0.855	–0.137	0.589	0.194	0.441
δ_{R0}	0.396	0.104	0.334	0.176	0.496	0.036	0.586	0.012
ΔV_{IP}	0.194	0.441	0.290	0.244	0.326	0.187	0.540	0.021
PI_{ABS}	–0.275	0.270	0.000	1.000	–0.100	0.694	0.279	0.261
PI_{total}	0.033	0.895	0.153	0.545	0.251	0.316	0.540	0.021
RC/CS_0	–0.164	0.514	0.108	0.670	–0.121	0.632	0.141	0.577

we did the measurements on the healthy looking tissues of those leaves. In many previous works, it was found that plants experiencing continuous salinity develop several mechanisms allowing to avoid oxidative stress, such as activation of signalling pathways that can enhance plant ability to stress tolerance, activation of antioxidant enzymes, accumulation of ROS-scavenging metabolites, such as ascorbate, glutathione, and tocopherols (Hanin *et al*. 2016). Fuhrer and Erismann (1980) found that in *Aesculus hippocastanum* growing in polluted areas, foliar Cl^- accumulations were less damaging in more severely polluted atmospheres. (*2*) The diminished performance of PSII might be evoked to a greater extent by other pollutants, such as heavy metals, sulphur oxides, nitrogen oxides, polycyclic aromatic hydrocarbons, and ozone being a consequence of heavy traffic (Wittmann *et al*. 2007, Pellegrini 2014, Popek *et al.* 2018) which are more important stressors during summer days.

The results of our examination showed that PSII performance in road-side leaves was indeed poorer than that in leaves from the opposite side of tree crowns. In most cases, the differences increased during the growing seasons. It should be concluded that there is a complex of traffic-born contamination responsible for disturbances in photosynthetic apparatus condition of street tree leaves.

The JIP-test used in our examination gave the first opportunity to see how deeply leaves of street trees are damaged by road-side contamination and what kind of damage can be found due to heavy pollution. The most affected structures and processes were the reaction centres of PSII and performance of electron carriers (plastoquinones). Performance of water-splitting complex was also diminished but only in particular cases. Leaf damages, which are visible to the naked eye, can be seen only in the late growing season. The JIP-test allowed us to ascertain that the unfavourable changes in photosynthetic apparatus arise since the beginning of the growing season and prolong or even increase during the summer. This indicates that environmental stress factors cumulate their effect gradually during the growing season.

References

Berkheimer S.F., Hanson E.: Deicing salts reduce cold hardiness and increase flower bud mortality of highbush blueberry. – J. Am. Soc. Hortic. Sci. **131**: 11-16, 2006.

Berkheimer S.F., Potter J.K., Andresen J.A., Hanson E.J.: Flower bud mortality and salt levels in highbush blueberry fields adjacent to Michigan highways treated with deicing salt. – HortTechnology **16**: 508-512, 2006.

Borowski J., Pstrągowska M.: Effect of street conditions, including saline aerosol, on growth of the small-leaved limes. – Rocznik Dendrologiczny **58**: 15-24, 2010.

Borowski J., Pstrągowska M., Swoczyna T.: Manifestations caused by salt aerosol on shoots and buds of street side limes. – In: Raček M. (ed.): Plants in Urban Areas and Landscape. Proceedings of the Scientific Papers. Pp. 3-6. Slovak University of Agriculture, Nitra 2014.

Brestič M., Živčák M.: PSII fluorescence techniques for measurement of drought and high temperature stress signal in crop plants: protocols and applications – In: Rout G.R., Das A.B. (ed.): Molecular Stress Physiology of Plants. Pp. 87-131. Springer, Dordrecht 2013.

Brestič M., Živčák M., Kalaji H.M. *et al*.: Photosystem II thermostability *in situ*: Environmentally induced acclimation and genotype-specific reactions in *Triticum aestivum* L. – Plant Physiol. Bioch. **57**: 93-105, 2012.

Bühler O., Nielsen C.N., Kristoffersen P.: Growth and phenology of established *Tilia cordata* street trees in response to different irrigation regimes. – Arboricult. Urban For. **32**: 3-9, 2006.

Bussotti F., Desotgiu R., Pollastrini M., Cascio C.: The JIP test: a tool to screen the capacity of plant adaptation to climate change. – Scand. J. Forest Res. **25**: 43-50, 2010.

Cekstere G., Nikodemus O., Osvalde A.: Toxic impact of the de-icing material to street greenery in Riga, Latvia. – Urban For. Urban Gree. **7**: 207-217, 2008.

Celestian S.B., Martin C.A.: Effects of parking lot location on size and physiology of four southwestern U.S. landscape trees. – J. Arboricult. **31**: 191-197, 2005.

Dmuchowski W., Badurek M.: Chloride and sodium in the leaves of urban trees in Warsaw in connection to their health condition. – Chemia i Inżynieria Ekologiczna **11**: 297-303, 2004.

Downton W.J.S.: Photosynthesis in salt-stressed grapevines. – Aust. J. Plant Physiol. **4**: 183-192, 1977.

Duan Y., Zhang M., Gao J. *et al.*: Thermotolerance of apple tree leaves probed by chlorophyll *a* fluorescence and modulated 820 nm reflection during seasonal shift. – J. Photoch. Photobio. B **152**: 347-356, 2015.

Dzierżanowski K., Popek R., Gawrońska H. *et al*.: Deposition of particulate matter of different size fractions on leaf surfaces and in waxes of urban forest species. **–** Int. J. Phytoremediat. **13**: 1037-1046, 2011.

Equiza M.A., Calvo-Polanco M., Cirelli D. *et al.*: Long-term impact of road salt (NaCl) on soil and urban trees in Edmonton, Canada. – Urban For. Urban Gree. **21**: 16-28, 2017.

Fini A., Ferrini F., Frangi P. *et al.*: Withholding irrigation during the establishment phase affected growth and physiology of Norway maple (*Acer platanoides*) and linden (*Tilia* spp.). – Arboricult. Urban For. **35**: 241-251, 2009.

Fuhrer J., Erismann K.H.: Tolerance of *Aesculus hippocastanum* L. to foliar accumulation of chloride affected by air pollution. – Environ. Pollut. A: **21**: 249-254, 1980.

Fung L.E., Wang S.S., Altman A, Hütterman A.: Effect of NaCl on growth, photosynthesis, ion and water relations of four poplar genotypes. – Forest Ecol. Manag. **107**: 135-146, 1998.

Gillner S., Vogt J., Tharang A. *et al.*: Role of street trees in mitigating effects of heat and drought at highly sealed urban sites. – Landscape Urban Plan. **143**: 33-42, 2015.

Goltsev V., Zaharieva I., Chernev P. *et al*.: Drought-induced modifications of photosynthetic electron transport in intact leaves: Analysis and use of neural networks as a tool for a rapid non-invasive estimation. – BBA-Bioenergetics **1817**: 1490-1498, 2012.

Guo Y.Y., Yu H.Y., Kong D.S. *et al.*: Effects of drought stress on growth and chlorophyll fluorescence of *Lycium ruthenicum* Murr. seedlings. – Photosynthetica **54**: 524-531, 2016.

Gupta B., Haung B.: Mechanism of salinity tolerance in plants: physiological, biochemical, and molecular characterization. – Int. J. Genomics **2014**: 701596, 2014.

Hanin M., Ebel C., Ngom M. *et al*.: New insights on plant salt tolerance mechanisms and their potential use for breeding. – Front. Plant Sci. **7**: 1787, 2016.

Hanslin H.M.: Short-term effects of alternative de-icing chemicals on tree sapling performance. – Urban For. Urban Gree. **10**: 53-59, 2011.

Headley D.B., Bassuk N.: Effect of time and application of sodium chloride in the dormant season on selected tree

seedlings. – J. Environ. Hortic. **9**: 130-136, 1991.
Hermans C., Smeyers M., Rodriguez R.M. e*t al*.: Quality assessment of urban trees: A comparative study of physiological characterisation, airborne imaging and on site fluorescence monitoring by the OJIP-test. – J. Plant Physiol. **160**: 81-90, 2003.
Hofstra G., Lumis G.P.: Levels of de-icing salt producing injury on apple trees. – Can. J. Plant Sci. **55**: 113-115, 1975.
Hu Y., Schmidhalter U.: Drought and salinity: a comparison of their effects on the mineral nutrition of plants. – J. Plant Nutr. Soil Sc. **168**: 541-549, 2005.
Jiang C.-D., Shi L., Gao H.-Y. *et al.*: Development of photosystems 2 and 1 during leaf growth in grapevine seedlings probed by chlorophyll *a* fluorescence transient and 820 nm transmission *in vivo*. – Photosynthetica **44**: 454-463, 2006.
Johnstone D., Tausz M., Moore G., Nicolas M.: Bark and leaf chlorophyll fluorescence are linked to wood structural changes in *Eucalyptus saligna*. – AoB Plants **6**: plt057, 2014.
Jonsson T.H.: Terminal bud failure of black cottonwood (*Populus trichocarpa*) exposed to salt-laden winter storms. – Tree Physiol. **26**: 905-914, 2006.
Kalaji H.M, Račková L., Paganová V. *et al.*: Can chlorophyll-*a* fluorescence parameters be used as bio-indicators to distinguish between drought and salinity stress in *Tilia cordata* Mill? – Environ. Exp. Bot. **152**: 149-157, 2018a.
Kalaji H.M., Oukarroum A., Alexandrov V. *et al.*: Identification of nutrient deficiency in maize and tomato plants by *in vivo* chlorophyll a fluorescence measurements. – Plant Physiol. Bioch. **81**: 16-25, 2014a.
Kalaji H.M., Rastogi A., Živčák M. *et al.*: Prompt chlorophyll fluorescence as a tool for crop phenotyping: an example of barley landraces exposed to various abiotic stress factors. – Photosynthetica **56**: 953-961, 2018b.
Kalaji H.M., Schansker G., Ladle R.J. *et al.*: Frequently asked questions about *in vivo* chlorophyll fluorescence: practical issues. – Photosynth. Res. **122**: 121-158, 2014b.
Kalaji M.H., Pietkiewicz S.: Salinity effects on plant growth and other physiological processes. – Acta Physiol. Plant. **15**: 89-124, 1993.
Lin M.Z., Jin M.F.: Soil Cu contamination destroys the photosynthetic systems and hampers the growth of green vegetables. – Photosynthetica **56**: 1336-1345, 2018.
Majewski G., Rogula-Kozłowska W.: The elemental composition and origin of fine ambient particles in the largest Polish conurbation: First results from the short-term winter campaign. – Theor. Appl. Climatol. **125**: 79-92, 2016.
Marosz A.: Soil pH, electrical conductivity values and roadside leaf sodium concentration at three sites in central Poland. – Dendrobiology **66**: 49-54, 2011.
Mathur S., Jajoo A.: Alterations in photochemical efficiency of photosystem II in wheat plant on hot summer day. – Physiol. Mol. Biol. Pla. **20**: 527-531, 2014.
Mehta P., Allakhverdiev S.I., Jajoo A.: Characterization of photosystem II heterogeneity in response to high salt stress in wheat leaves (*Triticum aestivum*). – Photosynth. Res. **105**: 249-255, 2010.
Misra A.N., Srivastava A., Strasser R.J.: Utilization of fast chlorophyll *a* fluorescence technique in assessing the salt/ion sensitivity of mung bean and *Brassica* seedlings. – J. Plant Physiol. **158**: 1173-1181, 2001.
Munns R., Tester M.: Mechanisms of salinity tolerance. – Annu. Rev. Plant Biol. **59**: 651-681, 2008.
Negrão S., Schmöckel S.M., Tester M.: Evaluating physiological responses of plants to salinity stress. – Ann. Bot.-London **119**: 1-11, 2017.
Nowak D.J., Crane D.E.: Carbon storage and sequestration by urban trees in the USA. – Environ. Pollut. **116**: 381-389, 2002.
Paludan-Müller G., Saxe H., Pedersen L.B., Randrup T.B.: Differences in salt sensivity of four deciduous tree species to soil or airborne salt. – Physiol. Plantarum **114**: 223-230, 2002.
Pellegrini E.: PSII photochemistry is the primary target of oxidative stress imposed by ozone in *Tilia americana.* – Urban For. Urban Gree. **13**: 94-102, 2014.
Percival G.C., Keary I.P., Al-Habsi S.: An assessment of the drought tolerance of *Fraxinus* genotypes for urban landscape plantings. – Urban For. Urban Gree. **5**: 17-27, 2006.
Pollastrini M., Holland V., Brüggeman W. *et al.*: Interaction and competition processes among tree species in young experimental mixed forests, assessed with chlorophyll fluorescence and leaf morphology. – Plant Biol. **16**: 323-331, 2014.
Pollastrini M., Holland V., Brüggemann W. *et al.*: Taxonomic and ecological relevance of the chlorophyll a fluorescence signature of tree species in mixed European forests. – New Phytol. **212**: 51-65, 2016.
Popek R., Przybysz A., Gawrońska H. *et al*.: Impact of particulate matter accumulation on the photosynthetic apparatus of roadside woody plants growing in the urban conditions. – Ecotox. Environ. Safe. **163**: 56-62, 2018.
Rogula-Kozłowska W., Majewski G., Widziewicz K. *et al*.: Seasonal variations of PM_1-bound water concentration in urban areas in Poland. – Atmos. Pollut. Res. **10**: 267-273, 2019.
Shashua-Bar L., Hoffman M.E.: Vegetation as a climatic component in the design of an urban street: An empirical model for predicting the cooling effect of urban green areas with trees. – Energ. Buildings **31**: 221-235, 2000.
Sieghardt M., Mursch-Radlgruber E., Paoletti E. *et al*.: The abiotic urban environment: Impact of urban growing conditions on urban vegetation. – In: Konijnendijk C.C., Nilsson K., Randrup T.B., Schipperijn J. (ed.): Urban Forests and Trees. Pp. 281-323. Springer, Berlin-Heidelberg 2005.
Srivastava A., Strasser R.J.: Stress and stress management of land plants during a regular day. – J. Plant Physiol. **148**: 445-455, 1996.
Strasser R.J., Govindjee: On the O-J-I-P fluorescence transient in leaves and Dl mutants of *Chlamydomonas reinhardtii*. – In: Murata N. (ed): Research in Photosynthesis. Vol. 4. Pp. 29-32. Kluwer Academic Publishers, Dordrecht 1992.
Strasser R.J., Srivastava A., Tsimilli-Michael M.: The fluorescence transient as a tool to characterize and screen photosynthetic samples. – In: Yunus M., Pathre U., Mohanty P. (ed.): Probing Photosynthesis: Mechanisms, Regulation and Adaptation. Pp. 445-483. Taylor & Francis, London 2000.
Strasser R.J., Tsimilli-Michael M., Qiang S., Goltsev V.: Simultaneous *in vivo* recording of prompt and delayed fluorescence and 820-nm reflection changes during drying and after rehydration of the resurrection plant *Haberlea rhodopensis*. – BBA-Bioenergetics **1797**: 1313-1326, 2010.
Strasser R.J., Tsimilli-Michael M., Srivastava A.: Analysis of the chlorophyll *a* fluorescence transient. – In: Papageorgiou G.C., Govindjee (ed.): Chlorophyll *a* Fluorescence: A Signature of Photosynthesis. Advances in Photosynthesis and Respiration. Pp. 321-362. Springer, Dordrecht 2004.
Strauss A.J., Krüger G.H.J, Strasser R.J., Van Heerden P.D.R.: Ranking of dark chilling tolerance in soybean genotypes probed by the chlorophyll *a* fluorescence transient O-J-I-P. – Environ. Exp. Bot. **56**: 147-157, 2006.
Sung J.H., Je S.M., Kim S.H., Kim Y.K.: [Effect of calcium chloride ($CaCl_2$) on chlorophyll fluorescence image and photosynthetic apparatus in the leaves of *Prunus sargentii*.] – J. Korean For. Soc. **99**: 922-928, 2010. [In Korean]
Swoczyna T., Kalaji H.M., Pietkiewicz S., Borowski J.: Ability

of various tree species to acclimation in urban environments probed with the JIP-test. – Urban For. Urban Gree. **14**: 544-553, 2015.

Swoczyna T., Łata B., Stasiak A. *et al*.: JIP-test in assessing sensitivity to nitrogen deficiency in two cultivars of *Actinidia arguta* (Siebold et Zucc.) Planch. ex Miq. – Photosynthetica **57**: 646-658, 2019.

Swoczyna T., Latocha P.: Durability of 28 ground-covering woody species and cultivars in road-side planting in Warsaw, Poland. – Acta Hortic. Regiotecturae **2**: 38-41, 2016.

Tabatabaei S.J.: Effect of salinity and N on the growth, photosynthesis and N status of olive (*Olea europaea* L.) trees. – Sci. Hortic.-Amsterdam **108**: 432-438, 2006.

Tyrväinen L., Pauleit S., Seeland K. *et al*.: Benefits and uses of urban forests and trees. – In: Konijnendijk C., Nilsson K., Randrup T., Schipperijn J. (ed.): Urban Forests and Trees. Pp. 81-114. Springer, Berlin-Heidelberg 2005.

van der Zee S.E.A.T.M., Shah S.H.H., Vervoort R.W. *et al*.: Root zone salinity and sodicity under seasonal rainfall due to feedback of decreasing hydraulic conductivity. – Water Resour. Res. **50**: 9432-9446, 2014.

Wang R., Chen S., Deng L. *et al.*: Leaf photosynthesis, fluorescence response to salinity and the relevance to chloroplast salt compartmentation and anti-oxidative stress in two poplars. – Trees **21**: 581, 2007.

Wang Z.X., Chen L., Ai J. *et al*.: Photosynthesis and activity of photosystem II in response to drought stress in Amur Grape (*Vitis amurensis* Rupr.). – Photosynthetica **50**: 189-196, 2012.

Wittmann C., Matyssek R., Pfanz H., Humar M.: Effects of ozone impact on the gas exchange and chlorophyll fluorescence of juvenile birch stems (*Betula pendula* Roth.). – Environ. Pollut. **150**: 258-266, 2007.

Yunusa A., Linatoc A.: Inventory of vegetation and assessment of carbon storage capacity towards a low carbon campus: a case study of Universiti Tun Husein Onn Malaysia, Johor Malaysia. – Traektoriâ Nauki **4**: 3001-3006, 2018.

Živčák M., Brestič M., Kunderlíková K. *et al.*: Repetitive light pulse-induced photoinhibition of photosystem I severely affects CO_2 assimilation and photoprotection in wheat leaves. – Photosynth. Res. **126**: 449-463, 2015b.

Živčák M., Brestič M., Kunderlíková K. *et al.*: Effect of photosystem I inactivation on chlorophyll *a* fluorescence induction in wheat leaves: Does activity of photosystem I play any role in OJIP rise? – J. Photoch. Photobio. B **152**: 318-324, 2015a.

Živčák M., Olšovská K., Slamka P. *et al.*: Application of chlorophyll fluorescence performance indices to assess the wheat photosynthetic functions influenced by nitrogen deficiency. – Plant Soil Environ. **5**: 210-215, 2014.

Appendix. Selected JIP-test parameters calculated on the basis of fast fluorescence kinetics.

Fluorescence parameters	Description
$F_0 = ABS/CS_0$	initial fluorescence obtained from measurements denoted also as ABS/CS_0
$F_K = F_{300}$	fluorescence at 300 μs after illumination of a dark-adapted sample
$F_J = F_{2ms}$	fluorescence at 2 ms after illumination of a dark-adapted sample
$F_I = F_{30ms}$	fluorescence at 30 ms after illumination of a dark-adapted sample
F_m	maximum fluorescence after illumination of a dark-adapted sample
$V_K = (F_{300} - F_0)/(F_m - F_0)$	relative variable fluorescence at 300 μs after illumination of a dark-adapted sample
$V_J = (F_{2ms} - F_0)/(F_m - F_0)$	relative variable fluorescence at 2 ms after illumination of a dark-adapted sample
$V_I = (F_{30ms} - F_0)/(F_m - F_0)$	relative variable fluorescence at 30 ms after illumination of a dark-adapted sample
V_K/V_J	efficiency of electron flow from OEC to PSII reaction centres
$M_0 = 4\ (F_{300} - F_0)/(F_m - F_0)$	approximated initial slope of the fluorescence transient, expressing the rate of RCs' closure
$F_v/F_m = \varphi_{P0} = TR_0/ABS = (F_m - F_0)/F_m$	maximum quantum yield of PSII photochemistry
$\psi_0 = ET_0/TR_0 = (F_m - F_{2ms})/(F_m - F_0) = 1 - V_J$	efficiency (probability) of an electron movement into the electron transport chain beyond Q_A
$\delta_{R0} = RE_0/ET_0 = (F_m - F_{2ms})/(F_m - F_0)$	probability that an electron from the intersystem electron carriers is transferred to reduce end electron acceptors at the PSI acceptor side
$RC/ABS = \gamma_{RC}/(1 - \gamma_{RC}) = \varphi_{P0}\ (V_J/M_0)$	Q_A reducing RCs per PSII antenna chlorophyll
$RC/CS_0 = \varphi_{P0}\ (V_J/M_0)\ (ABS/CS_0)$	density of active RCs (Q_A reducing RCs) per cross section at point 0
$PI_{ABS} = RC/ABS \times \varphi_{P0}/(1 - \varphi_{P0}) \times \psi_{E0}/(1 - \psi_{E0})$	performance index (potential) for energy conservation from photons absorbed by PSII to the reduction of intersystem electron acceptors
$PI_{total} = RC/ABS \times \varphi_{P0}/(1 - \varphi_{P0}) \times \psi_{E0}/(1 - \psi_{E0}) \times \delta_{R0}/(1 - \delta_{R0})$	performance index (potential) for energy conservation from photons absorbed by PSII to the reduction of PSI end electron acceptors